Efficient Computational Methods for Accurately Predicting Reduction Potentials of Organic Molecules

Amy L. Speelman and Jason G. Gillmore*

Department of Chemistry, Hope College, 35 E. 12th St., Holland, Michigan 49422-9000

Received: January 26, 2008; Revised Manuscript Received: April 16, 2008

A simple computational approach for predicting ground-state reduction potentials based upon gas phase geometry optimizations at a moderate level of density functional theory followed by single-point energy calculations at higher levels of theory in the gas phase or with polarizable continuum solvent models is described. Energies of the gas phase optimized geometries of the S_0 and one-electron-reduced D_0 states of 35 planar aromatic organic molecules spanning three distinct families of organic photooxidants are computed in the gas phase as well as well in implicit solvent with IPCM and CPCM solvent models. Correlation of the $D_0 - S_0$ energy difference (essentially an electron affinity) with experimental reduction potentials from the literature (in acetonitrile vs SCE) within a single family, or across families when solvent models are used, yield correlations with r^2 values in excess of 0.97 and residuals of about 100 mV or less, without resorting to computationally expensive vibrational calculations or thermodynamic cycles.

Introduction

The ground-state reduction potential of an organic molecule, $E°_{red}$, is an important descriptor of the molecule's electrochemical reactivity, describing its ability to accept an electron in solution. $E°_{red}$, along with the excited-state energy, determines the excited-state reduction potential which describes a molecule's potential photooxidizing power. In our group, we design novel photooxidants for eventual materials science applications. Through structural modifications, varying organic functional groups or heteroatom substitution, it is possible to produce desired changes in a molecule's redox properties. While the direction and rough magnitude of the change in $E°_{red}$ brought about by a particular structural modification can be estimated on the basis of a qualitative understanding of electronic structural factors that impact redox properties, a more accurate quantitative prediction of the magnitude of the change in $E°_{red}$ can be made using quantum mechanical calculations.

Methods for the direct computation of $E°_{red}$ typically involve a thermodynamic cycle, in which the gas phase free-energy difference between the ground state (S_0) and the corresponding one-electron reduced form (D_0) of a molecule and the free energy of solvation for each species are used to calculate the free energy change of the redox process in solution. The absolute redox potential is then computed from the free energy change. This absolute redox potential is corrected to an experimentally meaningful reduction potential relative to a reference electrode (e.g., the normal hydrogen electrode, NHE, or saturated calomel electrode, SCE).[1–4] Although this method has been proven to give accurate values in many cases, it can be computationally expensive to obtain such values, particularly for large molecules, as vibrational calculations to account for thermal/entropic contributions are strictly required, though perhaps not absolutely necessary.[2] A simpler method that can be used on molecules of variable size and structural complexity is thus desirable. We also find it conceptually appealing to avoid applying the large "correction" necessary to normalize to the NHE (or other reference electrode) and account for the energetics of the "free" electron. We therefore prefer a direct correlation of a computed energy difference to an experimental reduction potential, where this "correction" to a reference electrode is in effect a fitted parameter (as an intercept in the correlation).

Because it is a measure of a molecule's ability to accept an electron and move from the S_0 state to the corresponding one-electron-reduced D_0 state, $E°_{red}$ is closely related to the energy difference between a molecule's S_0 and D_0 states. This is a relatively simple quantity to compute (essentially an electron affinity). Neglecting solvent stabilization will have a dramatic effect on this energy difference, as solvent stabilization of the reduced species (D_0, an anion radical presuming S_0 is neutral) is very important to solution electrochemistry. Nevertheless, correlations of experimental $E°_{red}$ values to the corresponding electron affinity as computed in the gas phase that result in a good linear fit are possible (and should provide a reasonable means of predicting other unknown $E°_{red}$), provided that the solvent stabilization of D_0 relative to S_0 is similar for all molecules. This may be the case when the molecules being considered are closely related in structure such that solvent stabilization of D_0, while still important, is similar for all closely related molecules and can be accounted for by correlation with experimental reduction potentials as a contributor to the linear fit. However, for molecules with significant structural differences, the energetic effects of solvation are likely to vary considerably. Therefore, in order to create a global model valid for a broad range of molecules, solvent effects must be accounted for. This is most easily accomplished using a simple implicit solvent model. Using such a model to obtain molecular energies in solution, it should be possible to predict $E°_{red}$ values for a diverse set of organic structures.

Our particular interest is in the design of new photooxidants, and we desire a quantitative tool for predicting the redox properties of new compounds. $E°_{red}$ is a key component (along with excitation energy) of the excited-state reduction potential, $E*_{red}$, which ultimately determines a molecule's photooxidizing capability. We chose to begin with computing $E°_{red}$ because it varies to a greater extent and less predictably with substitution

* Corresponding author. E-mail: gillmore@hope.edu. Phone: 616-395-7308. Fax: 616-395-7118.

10.1021/jp800782e CCC: $40.75
Published on Web 06/19/2008

than excitation energy does, and can be computed using only ground-state methods. In this study we report our computation of the $D_0 - S_0$ energy difference, both in the gas phase and with two different solvent models, of three very different families of organic photooxidants (35 compounds in all), and the correlation of this energy difference with experimental ground-state reduction potentials.

Computational Details

All calculations were carried out using the Gaussian 03[5] or QChem[6] software packages. Density functional theory (DFT) with the Becke 3 Lee, Yang, and Parr (B3LYP) hybrid functional[7–9] was used for both geometry optimizations and molecular energy calculations. Optimal geometries were computed for each molecule in both its S_0 and one-electron-reduced D_0 forms in the gas phase using the MIDI! basis set, which has been optimized to provide accurate geometries for both neutral and charged organic molecules at low computational cost.[10,11] Molecular energies in these optimized geometries were computed using the 6-311+G(d,p) basis set, which includes diffuse functions in order to account for the energy of the loosely bound additional electron in the reduced species.[1]

Although molecular geometries should be relatively insensitive to solvent effects in organic solution, solvent stabilization cannot be neglected in considering relative energies. One of the most common methods to implicitly account for solvent effects is the polarizable continuum model (PCM), in which the solvent is modeled as a continuous static medium characterized by a dielectric constant, ϵ.[12,13] Two implementations using the PCM framework available in Gaussain 03 were used in the current study. The first, the conductor-like polarizable continuum model (CPCM),[14] is an implementation of the conductor-like screening model (COSMO)[15] in the PCM framework. In this approach a scaled conductor boundary condition, rather than a dielectric boundary condition, is used. In the second PCM implementation we examined, the isodensity polarizable continuum model (IPCM), a dielectric boundary condition is used, but the molecular cavity is defined by a calculation of the gas phase isodensity surface, rather than being constructed from overlapping spheres 120% of the van der Waal's radii.[16] Molecular energies of the gas phase optimized S_0 and D_0 geometries were computed in acetonitrile ($\epsilon = 36.64$)[5] at the B3LYP/6-311+G(d,p) level using each of these models.

These computational results were correlated with experimental $E°_{red}$ values as described in the following section to develop a method for predicting reduction potentials on the basis of the computed energies of D_0 and S_0.

Results and Discussion

The molecules considered in this study (Figure 1) represent three structurally distinct families of organic photooxidants: cyanoaromatics (**1**−**13**), quinones (**14**−**26**), and *N*-methyl heteroaromatic cations (NMHACs, **27**−**35**). By examining the strength of the correlation between the $D_0 - S_0$ energy differences and experimental $E°_{red}$ values for the molecules, both in their respective families and globally, the viability of this method as a predictive tool for the design of new compounds with desired reduction potentials can be evaluated.

By plotting (Figures 2 and 3) experimental reduction potential (x, in V vs reference electrode, SCE in our case) versus the computed energy difference (y, in eV) and performing a linear least-squares analysis, one obtains an equation in linear form (Table 1), where the slope (m) is in units of eV/V and the intercept (b) is in units of eV. To calculate a predicted $E°_{red}$

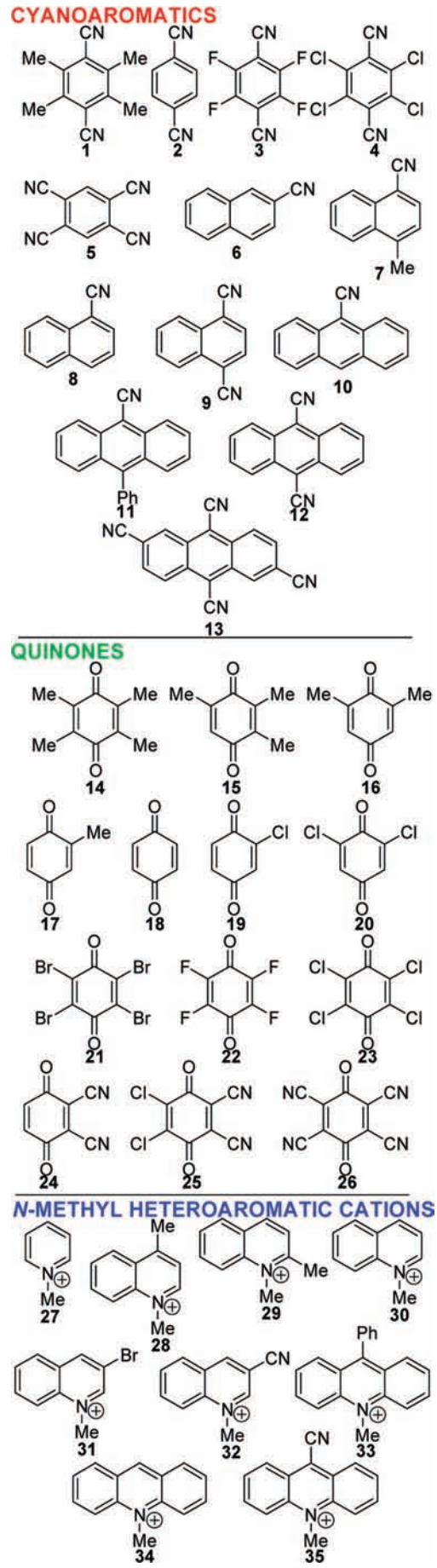

Figure 1. Cyanoaromatic molecules, quinones, and *N*-methyl heteroaromatic cations examined in this study.

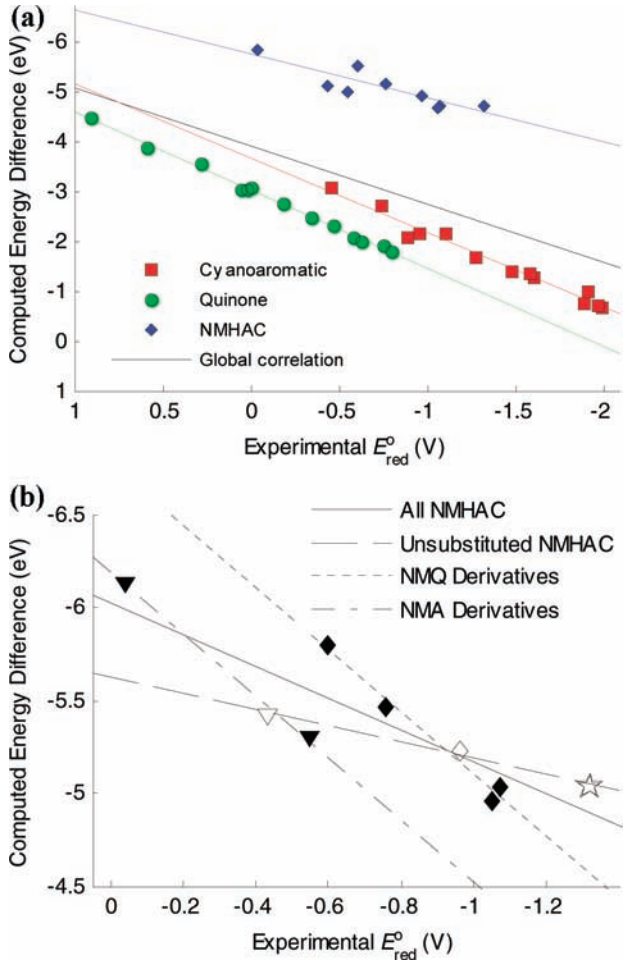

Figure 2. (a) Correlation of computed $D_0 - S_0$ energy difference at the B3LYP/6-311+G(d,p) level in the gas phase to experimental reduction potential. The global trendline is shown along with trendlines for each family of molecules. (b) An enlargement of the *N*-methyl heteroaromatic cation (NMHAC) region showing the overall "family" correlation and the correlations for each subfamily: *N*-methylquinoliniums (compounds **28**−**32**, plotted as filled and open diamonds), *N*-methylacridiniums (**33**−**35**, down triangles), or the three unsubstituted NMHACs (**27**, **30**, and **34**, three open symbols).

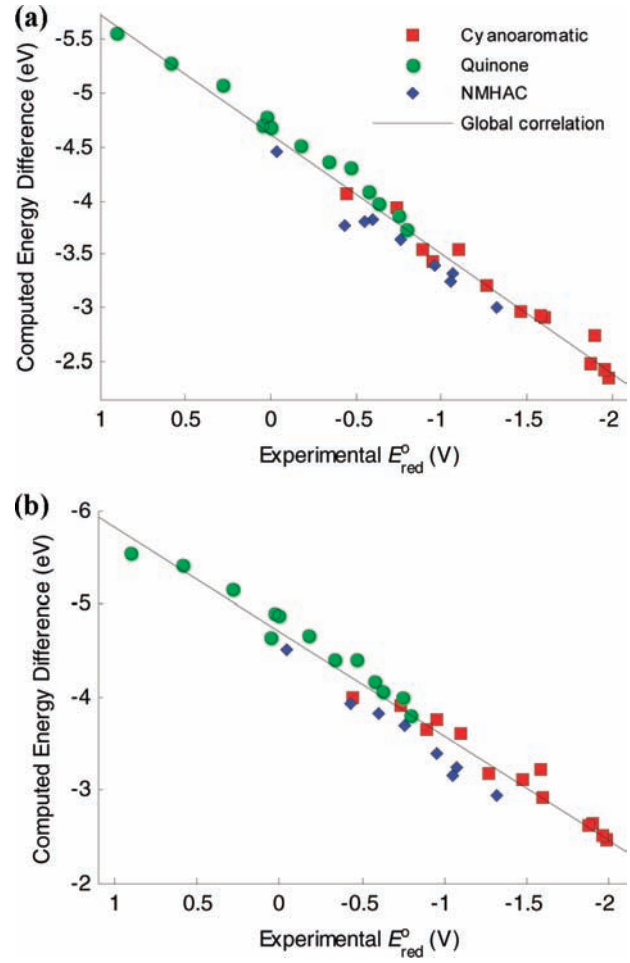

Figure 3. Correlation of computed $D_0 - S_0$ energy difference at the B3LYP/6-311+G(d,p) level to experimental E°_{red} showing the global correlation when (a) CPCM or (b) IPCM methods are used to account for solvation. The individual family trendlines for these methods (parameters in Table 1; plots in the Supporting Information) closely converge on these global trendlines.

from a computed $D_0 - S_0$ energy difference, the linear fit parameters are simply rearranged such that $x = (y - b)/m$. That is, for a new molecule, it is possible to calculate a predicted reduction potential from the computed $D_0 - S_0$ energy difference (E_{QM}), using the appropriate slope and intercept from Table 1, according to eq 1:

$$E^{\circ}_{red} = (E_{QM} - b)/m \quad (1)$$

Equation 1 also allows predicted reduction potentials to be calculated for each individual molecule used to establish the linear correlation (Table 1) in the first place. This allows each prediction to be compared to the experimental value from the literature as a residual. In aggregate (as a root-mean-square deviation, Table 2) these residuals are a measure of the validity of the model. Moreover, the computed *x*-intercept ($-b/m$) should correspond to the reference (SCE) potential for correlations that account for stabilization of ions by solvation. In correlations of experimental E°_{red} to gas phase energy differences, this intercept will also have a component that accounts for the unequal solvent stabilization of D_0 and S_0.

There is a very strong linear correlation between the $D_0 - S_0$ energy difference and E°_{red} for both the cyanoaromatics and the quinones, individually, even without incorporating solvent effects (Figure 2a and Table 1). The correlation is not as strong for the NMHACs, which indicates that these molecules are structurally dissimilar enough to prevent their grouping as a single family for our purposes. However, when the NMHAC set is further broken down based on the parent molecule (Figure 2b), strong linear correlations are again observed for the derivatives of *N*-methylquinolinium (**28**−**32**) and the derivatives of *N*-methylacridinium (**33**−**35**) when they are considered separately. Likewise, when only the unsubstituted *N*-methylpyridinium, quinolinium, and acridinium molecules are considered (**27**, **30**, and **34**), the correlation is again strong. The appearance of a separate trendline for each of the different families (or NMHAC subfamilies) demonstrates that while the relative energetic effects of solvation within a family are similar, they can vary considerably across families. Moreover, what constitutes a "family" is not always as readily predicted as one might hope.

When the CPCM (Figure 3a) and IPCM (Figure 3b) methods are used to account for solvation, the separate trendlines present in the gas phase for the NMHAC subfamilies completely collapse to a single line with a strong r^2 value. Moreover, the separate trendlines for each individual family (while still present, Table 1) converge on a single global trendline with reasonably small residuals and a good r^2 value. This global trendline is of

TABLE 1: Fit Parameters for Correlations of E°_{red} to $D_0 - S_0$ Energy Difference Based on Family and Global Trendlines

family	solvent model	slope m (eV/V)	y-intercept b (eV)	r^2	rmsd[a] residuals (V)	x-intercept (V)[b]
cyanoaromatics	gas phase	−1.4959	−3.6562	0.9758	0.0769	
cyanoaromatics	CPCM	−1.0886	−4.6067	0.9651	0.0929	−4.23
cyanoaromatics	IPCM	−1.0508	−4.6291	0.9577	0.1026	−4.41
quinones	gas phase	−1.5741	−3.0185	0.9970	0.0273	
quinones	CPCM	−1.0528	−4.6908	0.9852	0.0613	−4.46
quinones	IPCM	−1.0274	−4.7608	0.9605	0.1015	−4.63
NMHACs	gas phase	−0.8623	−6.0245	0.7676	0.2035	
unsubstituted	gas phase	−0.4358	−5.6221	0.9872	0.0416	
NMQ derivatives	gas phase	−1.6688	−6.7784	0.9778	0.0273	
NMA derivatives	gas phase	−1.6628	−6.1852	0.9913	0.0204	
NMHACs	CPCM	−1.0714	−4.4173	0.9650	0.0704	−4.12
NMHACs	IPCM	−1.2160	−4.5283	0.9869	0.0444	−3.72
all	gas phase	−1.1715	−3.9016	0.2554	1.1994	
all	CPCM	−1.1214	−4.6193	0.9730	0.1171	−4.12
all	IPCM	−1.1223	−4.6812	0.9593	0.1466	−4.17

[a] Root-mean-square deviation, taken from individual residuals for each compound as predicted by each trendline (as reported in Table 2 and in the Supporting Information). [b] Computed x-intercept ($= -b/m$) should roughly correspond to the reference electrode potential (SCE = NHE + 0.24 V = −4.12 V),[1,18] though this is only expected to be valid in solution, not gas phase.

TABLE 2: Comparison of Experimental E°_{red} to Calculated E°_{red} Using Family-Specific Correlations in the Gas Phase and Global Correlation with CPCM to Account for Solvation

	experimental		gas phase, by family		CPCM, global fit	
compound	literature E°_{red} (V)[a]	lit ref	calculated[b] E°_{red} (V)	residual (V)	calculated[c] E°_{red} (V)	residual (V)
1	−1.90	19	−1.780	0.120	−1.682	0.218
2	−1.60	20	−1.590	0.010	−1.525	0.075
3	−1.10	21	−1.024	0.076	−0.952	0.148
4	−0.95	21	−1.003	−0.053	−1.060	−0.110
5	−0.74	21	−0.623	0.117	−0.604	0.136
6	−1.98	22	−1.989	−0.009	−2.022	−0.042
7	−1.96	22	−1.969	−0.009	−1.962	−0.002
8	−1.88	22	−1.937	−0.057	−1.907	−0.027
9	−1.27	22	−1.335	−0.065	−1.264	0.006
10	−1.58	19	−1.548	0.032	−1.503	0.077
11	−1.47	23	−1.512	−0.042	−1.478	−0.008
12	−0.89	20	−1.056	−0.166	−0.952	−0.062
13	−0.45	20	−0.403	0.047	−0.485	−0.035
14	−0.80	24	−0.784	0.011	−0.785	0.010
15	−0.75	25	−0.719	0.031	−0.671	0.079
16	−0.63	24	−0.660	−0.030	−0.569	0.061
17	−0.58	25	−0.607	−0.027	−0.472	0.108
18	−0.47	24	−0.449	0.022	−0.266	0.205
19	−0.34	25	−0.351	−0.011	−0.224	0.116
20	−0.18	25	−0.181	−0.001	−0.083	0.097
21	0.00	25	0.023	0.023	0.064	0.064
22	0.02	24	0.015	−0.007	0.138	0.116
23	0.05	26	0.013	−0.037	0.077	0.027
24	0.28	25	0.326	0.046	0.406	0.126
25	0.59	26	0.548	−0.042	0.587	−0.003
26	0.90	26	0.920	0.020	0.840	−0.060
27	−1.32	27	−1.355	−0.035	−1.442	−0.122
28	−1.07	21	−1.049	0.021	−1.165	−0.095
29	−1.05	28	−1.088	−0.038	−1.219	−0.169
30	−0.96	28	−0.928	0.032	−1.083	−0.123
31	−0.76	28	−0.786	−0.026	−0.867	−0.107
32	−0.60	28	−0.589	0.011	−0.703	−0.103
33	−0.55	29	−0.529	0.021	−0.718	−0.168
34	−0.43	25	−0.458	−0.028	−0.758	−0.328
35	−0.04	30	−0.034	0.006	−0.144	−0.104

[a] vs SCE in CH_3CN (or corrected to vs SCE according to refs 18 and 31, for those not so reported in the primary reference). [b] Computed using gas phase family (or NMHAC subfamily) correlations from Table 1 according to eq 1. [c] Computed using CPCM global correlation from Table 1 according to eq 1.

particular use because it provides a simple, efficient method to predict the approximate magnitude of E°_{red} for new organic molecules of similar size, even those that do not belong to the families described herein.

The residuals on predicted E°_{red} are smallest when using fits based on family specific correlation to the gas phase calculations, but these correlations are highly dependent on properly defining and parameterizing the family. As observed with the NMHACs, determining what molecules constitute a family can be difficult. Thus when using this method, it is advisable to supplement it with at least one of the solvent-based models. In the solvent-based methods, the individual family trendlines again can

potentially give the most accurate predictions if sufficient members of a family are available to parameterize the correlation. However the separate family lines using solvation do converge on a single global trendline that spans these three structurally diverse families (and presumably other aromatic organic molecules). This allows the use of the global fit (i.e., eq 1 with $m = -1.1214$ eV/V and $b = -4.6193$ V for CPCM at the B3LYP/6-311+G(d,p) level) as a viable method for the prediction of $E°_{red}$ to within about 100 mV. Thus the solvent-based methods can aid the design of synthetic targets with desired redox properties, even if no close structural analogs are known. This is particularly valuable when $E°_{red}$ values for other members of a family are not available, as well as for the occasional user who may not choose to calibrate a correlation for a specific family of molecules.

In our experience, IPCM calculations are generally more difficult to converge and are considerably more computationally expensive than CPCM calculations. This is in agreement with the results of Cossi et al.[17] For example, the IPCM D_0 energy calculation for **33** failed to converge in our hands, and the S_0 energy calculation of **6** took about 10 times longer with IPCM than CPCM. In addition, the IPCM residuals are generally slightly larger when using the overall trendline, so of the two methods presented herein, the CPCM model should be used preferentially. Moreover, the computed *x*-intercepts (Table 2), which should correspond to the absolute potential of the reference electrode in the given solvent, are in best agreement with experimental values (NHE = −4.36 V; SCE = NHE + 0.2412 V = −4.12 V) for the CPCM models, particularly when the overall global trendline is used.[1,18]

Given the success of the global trendline derived from our CPCM calculations with the 6-311+G(d,p) basis set in predicting ground-state reduction potentials and an insightful reviewer comment suggesting that the diffuse functions of that basis set are likely most important for the gas phase calculations of the reduced D_0 species, we decided to repeat all our CPCM single point energy calculations with the 6-31G(d) and MIDI! basis sets (Figure 4) in an attempt to make our method even more computationally efficient. The linear fits of CPCM calculations using all three basis sets (MIDI!, 6-31G(d), and 6-311+G(d,p)) vs experimental $E°_{red}$ are compared in Table 3. Interestingly, the r^2 and rmsd residuals are as good or better with the smaller basis sets. Specifically, results using 6-31G(d) are consistently better than those using MIDI!, which are (rather surprisingly) roughly comparable to those using 6-311+G(d,p). The improvements in r^2 and rmsd residuals are admittedly fairly small, and not in and of themselves impressive. Nevertheless, this is a considerable advance due to the increase in the efficiency of the calculations for an empirically equally good or better result, as compute times for 6-31G(d) and MIDI! are relatively similar to one another and roughly an order of magnitude or more shorter than for 6-311+G(d,p). The control experiment using the smaller basis sets for the gas phase single point energies was also performed (see the Supporting Information), and confirmed that the diffuse functions of 6-311+G(d,p) are indeed somewhat important in the gas phase.

The one notable trade-off in switching away from the larger basis set is that the *x*-intercept no longer corresponds well to the reference potential, as it did very well for the 6-311+G(d,p) PCM global fits and reasonably well for most of the individual family fits save for the NMHACs with IPCM. This indicates that while the computed $D_0 - S_0$ energy difference found using either of the smaller basis sets with CPCM correlates very well with experimental reduction potential, there is a similar systemic

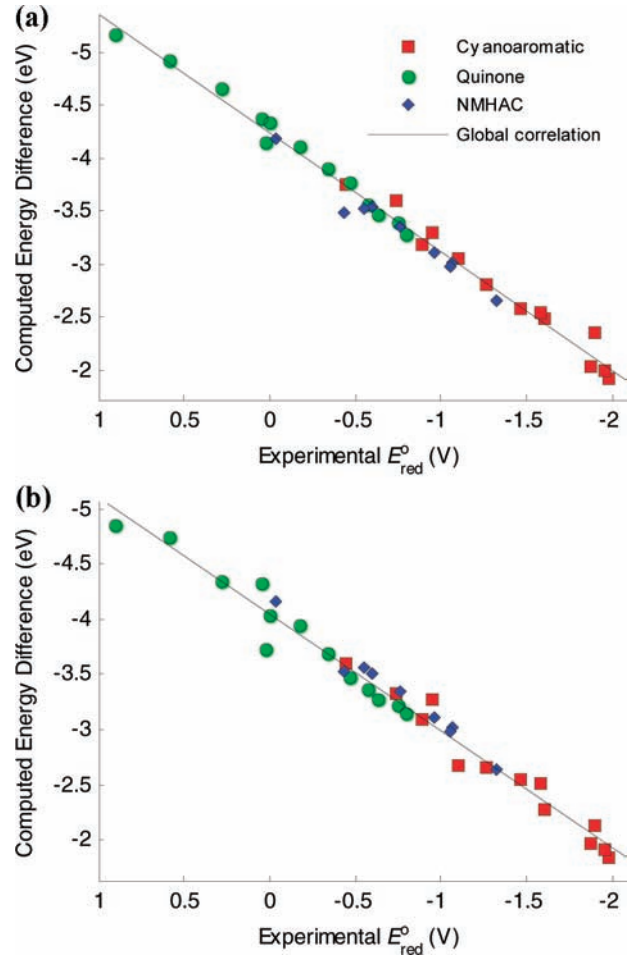

Figure 4. Correlation of computed $D_0 - S_0$ energy differences using CPCM methods to account for solvation with smaller basis sets (a) B3LYP/6-31G(d) and (b) B3LYP/MIDI!. The individual family trendlines for these methods (parameters in Table 3; plots in the Supporting Information) closely converge on these global trendlines, which in turn provide predictive abilities comparable to the larger B3LYP/6-311+G(d,p) basis set with the same solvent model (Figure 3a).

error introduced by using either of the smaller basis sets. This systemic error is corrected for in the intercept value in these fits, and so the predictive ability is still excellent but the intercept is no longer solely a correction to the reference potential. This unknown systemic error is absent when the larger basis set is employed, except perhaps in the NMHACs, and thus the *x*-intercepts obtained from the 6-311+G(d,p) data corresponds well to the SCE reference electrode of the experimental data.

For the casual user, gas phase geometry optimizations with B3LYP/MIDI! (or presumably 6-31G(d)) followed by single point CPCM energies with B3LYP/6-31G(d) will give good predictive ability across a broad range of molecules, while the more time-consuming B3LYP/6-311+G(d) single-point CPCM energy calculations remove the unspecified systemic error and provide the additional comfort of an *x*-intercept term that purely corrects for the chosen experimental reference electrode. Finally, when gas phase calculations are used, the diffuse functions of B3LYP/6-311+G(d,p) can improve the correlation relative to the smaller basis sets, but the use of the larger basis set completely offsets the time saved by not employing PCM solvent models.

As desired, the calculations are computationally efficient in that they can each be accomplished on a single 3.0 GHz Intel Xeon x86_64 processor in a reasonable amount of time. The

TABLE 3: Fit Parameters for Correlations of E°_{red} to $D_0 - S_0$ Energy Difference (Using the CPCM Solvent Model and Varying the Basis Set) Based on Family and Global Trendlines

family	B3LYP	slope *m* (eV/V)	*y*-intercept *b* (eV)	r^2	rmsd[a] residuals (V)	*x*-intercept (V)[b]
cyanoaromatics	MIDI!	−1.1172	−4.1256	0.9625	0.0964	−3.69
cyanoaromatics	6-31G(d)	−1.1699	−4.3354	0.9718	0.0832	−3.71
cyanoaromatics	6-311+G(d,p)	−1.0886	−4.6067	0.9651	0.0929	−4.23
quinones	MIDI!	−1.0729	−4.0138	0.9464	0.1192	−3.74
quinones	6-31G(d)	−1.1335	−4.2484	0.9862	0.0593	−3.75
quinones	6-311+G(d,p)	−1.0528	−4.6908	0.9852	0.0613	−4.46
NMHACs	MIDI!	−1.1087	−4.1526	0.9773	0.0563	−3.75
NMHACs	6-31G(d)	−1.1105	−4.1514	0.9662	0.0692	−3.74
NMHACs	6-311+G(d,p)	−1.0714	−4.4173	0.9650	0.0704	−4.12
all	MIDI!	−1.0600	−4.0518	0.9764	0.1093	−3.82
all	6-31G(d)	−1.1212	−4.2324	0.9859	0.0840	−3.78
all	6-311+G(d,p)	−1.1214	−4.6193	0.9730	0.1171	−4.12

[a] Root-mean-square deviation, taken from individual residuals for each compound as predicted by each trendline (as reported in the Supporting Information). [b] Computed *x*-intercept (= $-b/m$) corresponds to the reference electrode potential correction (SCE = NHE + 0.24 V = −4.12 V),[1,18] and any systematic inaccuracies of the computational model employed.

two geometry optimizations required for each molecule (S_0 and D_0) together took between a few minutes (e.g., for compounds **18**, **27**, etc.) to a few hours (**13**, **33**, etc.) to compute at the B3LYP/MIDI! level of theory. The pair of single-point energies computed for the two geometries at the B3LYP/6-31G(d) level of theory together took under 40 min for even the largest molecules, whether in the gas phase or with CPCM. At the highest level of theory used, B3LYP/6-311+G(d,p), the pair of gas phase single-point energies took from 3 min for the smallest molecules to a few hours for the largest, whereas those same two computations with CPCM solvent modeling required 20 min to 11 h. In all cases, any pair of computations (S_0 and D_0) of both geometry and energy could be completed in less than one full day, and for many of the smaller molecules could be completed in less than an hour. Thus the entire set of computations required to reproduce the full body of work reported herein (save for the less useful and more time-consuming IPCM calculations) could be done in a few weeks of compute time on a single processor.

Conclusions

We have successfully developed methods for the prediction of ground-state reduction potentials of organic molecules that have proven both accurate and computationally affordable. The method involves no vibrational calculations, fairly simple gas phase geometry optimizations, and higher level of theory single point energy calculations. The latter can be conducted with or without PCM solvent models, depending on the number of close structural analogs available to support the necessary correlation. Correlation to experiment is good, with r^2 values generally in excess of 0.97. Typical residuals for both family specific gas phase and PCM fits, as well as global fits using CPCM, are about 100 mV or less, which is sufficient to help direct synthetic efforts of new photooxidants. Moreover, as the computational methodology is easy to implement and not too expensive, particularly when CPCM calculations are carried out using the more modest 6-31G(d) basis set, this method should have broad appeal to the practicing organic chemist.

The molecules considered in this work are fairly rigid organic aromatic compounds, and centered on compounds of utility as photooxidants. More conformationally flexible molecules will be presented in a future report, as will a broader range of aromatic molecules that are less reducible than those presented herein. Our next goals will be to apply excited-state computational methods for the estimation of the $E_{0,0}$ nonvertical singlet excitation energy (of singlet photooxidants), as well as ground-state methods for the determination of triplet energies (for triplet photooxidants), to ultimately yield a suite of methods that will together enable the prediction of the excited-state reduction potentials that ultimately describe the photooxidizing power of a photooxidant.

Acknowledgment. This research was supported by a Hope College/HHMI Computational Science & Modeling Scholars Award, a Cottrell College Science Award from Research Corporation, and a Camille & Henry Dreyfus Foundation Startup Award. We also thank Hope College Professors Brent Krueger and William Polik and Mr. Paul Van Allsburg for advice and instruction on utilizing Hope's Computational Science & Modeling Laboratory, as well as helpful correspondence and feedback from Dr. David Giesen (Kodak Research Laboratories) and Professor Chris Cramer (University of Minnesota) on the preliminary results of this work. We also thank the reviewers of the initial manuscript for an insightful suggestion regarding the application of smaller basis sets to the PCM single-point calculations, and suggestions for clarifying the text and Figure 2b.

Supporting Information Available: Tables containing the complete computational details (including software used for each optimization and energy calculation, individual S_0 and D_0 energies, and predicted E°_{red} values for each molecule by each linear fit presented in Tables 1 and 3, with residuals); an additional version of Figures 3a, 3b, 4a, and 4b, containing individual family trendlines (as described in Tables 1 and 3), which demonstrate their close convergence upon the global trendline; the data for gas phase single-point energies using B3LYP/MIDI! and B3LYP/6-31G(d), which confirm that the diffuse functions in B3LYP/6-311+G(d,p) are important though not necessarily essential for gas phase calculations. This material is available free of charge via the Internet at http://pubs.acs.org.

References and Notes

(1) Cramer, C. J. *Essentials of Computational Chemistry: Theories and Models*, 2nd ed.; John Wiley & Sons, Ltd.: Chichester, West Sussex, England, 2007.

(2) Baik, M.-H.; Friesner, R. A. *J. Phys. Chem. A* **2002**, *106*, 7407.

(3) Schmidt am Busch, M.; Knapp, E.-W. *J. Am. Chem. Soc.* **2005**, *127*, 15730.

(4) Winget, P.; Weber, E. J.; Cramer, C. J.; Truhlar, D. G. *Phys. Chem. Chem. Phys.* **2000**, *2*, 1231.

(5) Frisch, M. J.; Trucks, G. W.; Schlegel, H. B.; Scuseria, G. E.; Robb, M. A.; Cheeseman, J. R.; Montgomery Jr., J. A.; Vreven, T.; Kudin, K. N.; Burant, J. C.; Millam, J. M.; Iyengar, S. S.; Tomasi, J.; Barone, V.; Mennucci, B.; Cossi, M.; Scalmani, G.; Rega, N.; Petersson, G. A.; Nakatsuji, H.; Hada, M.; Ehara, M.; Toyota, K.; Fukuda, R.; Hasegawa, J.; Ishida, M.; Nakajima, T.; Honda, Y.; Kitao, O.; Nakai, H.; Klene, M.; Li, X.; Knox, J. E.; Hratchian, H. P.; Cross, J. B.; Bakken, V.; Adamo, C.; Jaramillo, J.; Gomperts, R.; Stratmann, R. E.; Yazyev, O. ;Austin, A. J.; Cammi, R.; Pomelli, C.; Ochterski, J. W.; Ayala, P. Y.; Morokuma, K.; Voth, G. A.; Salvador, P.; Dannenberg, J. J.; Zakrzewski, V. G.; Dapprich, S.; Daniels, A. D.; Strain, M. C.; Farkas, O.; Malick, D. K.; Rabuck, A. D.; Raghavachari, K.; Foresman, J. B.; Ortiz, J. V.; Cui, Q.; Baboul, A. G.; Clifford, S.; Cioslowski, J.; Stefanov, B. B.; Liu, G.; Liashenko, A.; Piskorz, P.; Komaromi, I.; Martin, R. L.; Fox, D. J.; Keith, T.; Al-Laham, M. A.; Peng, C. Y.; Nanayakkara, A.; Challacombe, M.; Gill, P. M. W.; Johnson, B.; Chen, W.; Wong, M. W.; Gonzalez, C.; Pople, J. A. *Gaussian 03*, revision B.02; Gaussian, Inc.: Wallingford, CT, 2004.

(6) Shao, Y.; Fusti-Molnar, L.; Jung, Y.; Kussmann, J.; Ochsenfeld, C.; Brown, S. T.; Gilbert, A. T. B.; Slipchenko, L. V.; Levchenko, S. V.; O'Neill, D. P.; Distasio, R. A., Jr.; Lochan, R. C.; Wang, T.; Beran, G. J. O.; Besley, N. A.; Herbert, J. M.; Lin, C. Y.; Van Voorhis, T.; Chien, S. H.; Sodt, A.; Steele, R. P.; Rassolov, V. A.; Maslen, P. E.; Korambath, P. P.; Adamson, R. D.; Austin, B.; Baker, J.; Byrd, E. F. C.; Dachsel, H.; Doerksen, R. J.; Dreuw, A.; Dunietz, B. D.; Dutoi, A. D.; Furlani, T. R.; Gwaltney, S. R.; Heyden, A.; Hirata, S.; Hsu, C.-P.; Kedziora, G.; Khalliulin, R. Z.; Klunzinger, P.; Lee, A. M.; Lee, M. S.; Liang, W.; Lotan, I.; Nair, N.; Peters, B.; Proynov, E. I.; Pieniazek, P. A.; Rhee, Y. M.; Ritchie, J.; Rosta, E.; Sherrill, C. D.; Simmonett, A. C.; Subotnik, J. E.; Woodcock III, H. L.; Zhang, W.; Bell, A. T.; Chakraborty, A. K.; Chipman, D. M.; Keil, F. J.; Warshel, A.; Hehre, W. J.; Schaefer III, H. F.; Kong, J.; Kzrylov, A. I.; Gill, P. M. W.; Head-Gordon, M. *Phys. Chem. Chem. Phys* **2006**, *8*, 3172.

(7) Becke, A. D. *J. Chem. Phys.* **1996**, *104*, 1040.

(8) Becke, A. D. *Phys. Rev. A* **1988**, *38*, 3098.

(9) Lee, C.; Yang, W.; Parr, R. G. *Phys. Rev. B* **1988**, *37*, 785.

(10) Easton, R. E.; Giesen, D. J.; Welch, A.; Cramer, C. J.; Truhlar, D. G. *Theor. Chim. Acta* **1996**, *93*, 281.

(11) Li, J.; Cramer, C. J.; Truhlar, D. G. *Theor. Chem. Acc.* **1998**, *99*, 192.

(12) Miertuš, S.; Scrocco, E.; Tomasi, J. *Chem. Phys.* **198155**, 117.

(13) Cramer, C. J.; Truhlar, D. G. *Chem. Rev* **1999**, *99*, 2161.

(14) Barone, V.; Cossi, M. *J. Phys. Chem. A* **1998**, *102*, 1995.

(15) Klamt, A.; Schüürmann; J, *J. Chem. Soc., Perkin Trans. 2* **1993**, 799.

(16) Foresman, J. B.; Keith, T. A.; Wiberg, K. B.; Snoonian, J.; Frisch, M. J. *J. Phys. Chem.* **1996**, *100*, 16098.

(17) Cossi, M.; Barone, V.; Cammi, R.; Tomasi, J. *Chem. Phys. Lett.* **1996**, *255*, 327.

(18) Bard, A. J.; Faulkner, L. R. *Electrochemical Methods: Fundamentals and Applications*, 2nd ed.; John Wiley & Sons: New York, 2000.

(19) Ishiguro, K.; Nakano, T.; Shibata, H.; Sawaki, Y. *J. Am. Chem. Soc.* **1996**, *118*, 7255.

(20) Mattes, S. L.; Farid, S. In *Organic Photochemistry*; Padwa, A., Ed.; Marcel Dekker: New York, 1983; *Vol. 6*, p 233.

(21) Ohkubo, K.; Suga, K.; Morikawa, K.; Fukuzumo, S. *J. Am. Chem. Soc.* **2003**, *125*, 12850.

(22) Kiau, S.; Liu, G.; Shukla, D.; Dinnocenzo, J. P.; Young, R. H.; Farid, S. *J. Phys. Chem. A* **2003**, *107*, 3625.

(23) Lin, J.-H.; Elangovan, A.; Ho, T.-I. *J. Org. Chem.* **2005**, *70*, 7397.

(24) Frontana, C.; Vázquez, A.; Garza, J.; Vargas, R.; González, I. *J. Phys. Chem. A* **2006**, *110*, 9411.

(25) Fukuzumi, S.; Koumitsu, S.; Hironaka, K.; Tanaka, T. *J. Am. Chem. Soc.* **1987**, *109*, 305.

(26) Vazquez, C.; Calabrese, J. C.; Dixon, D. A.; Miller, J. S. *J. Org. Chem.* **1993**, *58*, 65.

(27) Lee, K. Y.; Kochi, J. K. *J. Chem. Soc., Perkin Trans. 2* **1992**, 1011.

(28) Fukuzumi, S.; Kitano, T. *J. Chem. Soc., Perkin Trans. 2* **1991**, 41.

(29) Fukuzimi, S.; Ohkubo, K.; Tokuda, Y.; Suenobu, T. *J. Am. Chem. Soc.* **2000**, *122*, 4286.

(30) Matern, A. I.; Yanilkin, V. V; Morosov, V. I.; Charushin, V. N.; Chupakhin, O. N. *Russ. Chem. Bull., Int. Ed.* **2006**, *55*, 1498.

(31) Pavlishchuk, V. V.; Addison, A. W. *Inorg. Chim. Acta* **2000**, *298*, 97.

JP800782E